Short Communication

Preparation of CF$_x$@C Microcapsules as a High-rate Capability Cathode of Lithium Primary Battery

Ling Zhu[1,2], Yong Pan[1,2,*], Lei Li[1,2], Jie Zhou[1,2], Weixin Lei[1,2,*], Jiahuang Deng[1,2], Zengsheng Ma[1,2]

[1] National-Provincial Laboratory of Special Function Thin Film Materials, Xiangtan 411105, Hunan, China
[2] School of Materials Science and Engineering, Xiangtan University, Xiangtan 411105, Hunan, China
[*]E-mail: ypan@xtu.edu.cn, wxlei@xtu.edu.cn

The Core-shell structure carbon-coated graphite fluoride (CF$_x$@C) microcapsules were prepared by microencapsulation and carbonization. The CF$_x$@C has a spherical shape and the carbon coating is constructed of thousands of carbon micro-shperes. With the exterior conductivity provided by the carbon coating, CF$_x$@C cathode achieves a higher energy density and a higher power density than the pristin CF$_x$. The energy density is increased from 505 Wh Kg^{-1} by CF$_x$ to 1171 Wh Kg^{-1} by CF$_x$@C at 0.5 C and the maximun discharge rate is improved from 0.5 C by CF$_x$ to 5 C by CF$_x$@C. Both fully discharged (at 0.1 C) pristin CF$_x$ and CF$_x$@C cathodes are studied to reveal the effect mechanism. The high power density is attributed to: 1) the enhanced combination of CF$_x$@C and acetylene black by plyurea guarantees the electrons transferring from Al collector to the surface of CF$_x$@C; 2) the carbon coating of CF$_x$@C with a good electronic conductivity accelerates the shift of electrons to the GIC interface; 3) the carbon coating which shows an porous surface enlarges the contact area and can store much electrolyte and allows more channels for the Li$^+$ ion transferring.

1. INTRODUCTION

Li/graphite fluoride (CF$_x$) batteries are known to have the highest theoretical specific capacity compared with other primary batteries and are got much attention in military, aerospace and advanced medical equipments. There are some unique advantages on Li/CF$_x$ cells, such as flat discharge potential, low self-discharge and wide operating temperature (-40 to 170 ℃)[1-3]. The overall discharge reaction of a Li/CF$_x$ battery can be expressed as "CF$_x$ + xLi → C + xLiF"[4]. Due to the

strong covalent bond C-F and the low electronic conductivity of CF_x, the cathode shows a significant polarization and leads to a much lower discharge voltage (around 2.4 V) than the open circuit voltage (3.2-3.5 V)[5].

In order to improve the rate capability of Li/CF_x battery, many efforts have been made. On the aspect of preparation, sub-fluorinated CF_x[6-9] and low temperature CF_x[10-13] were manufactured. However, their successes were made at a cost of specific capacity for the low fluorinated degree. Hybrid cathodes of CF_x and other materials were adopted in Li/CF_x battery[14-17]. Nonetheless, their improvement were limited. Surface modification is an effective way to change performances of materials[18-21], but there are relatively few researches on CF_x. Q. Zhang et al. prepared the carbon-coated CF_x by heat treating the mixture of CF_x with polyvinylidence difluoride (PVDF) and the rate capacity was improved, while the coated particles tended to aggregate[22].

Actually, carbon coating has been investigated on many electrode materials to enhance their electrochemical performances. Ho Chul Shin, et al. found that the electrochemical properties of $LiFePO_4$ could be improved by carbon coating for enhancing the electrical contacts [23]. Wei-Ming Zhang, et al. prepared the carbon coated Fe_3O_4 nanospindles as an anode material, of which the coulombic efficiency, cycling performance and rate capability were enhanced[24]. It was attributed to the carbon layer for increasing the electronic conductivity leading to the formation of uniform and thin solid electrolyte interphase (SEI) films. Mokhlesur Rahman, et al. did some research on amorphous carbon coated $Li_4Ti_5O_{12}$-TiO_2 as an anode material and discovered that the electrochemical performances can be improved by carbon layer for the grain boundary interface embedded carbon matrix can store electrolyte and allows more channels for the Li^+ ion[25]. S. Lee, et al. studied the carbon-coated single-crystal $LiMn_2O_4$ nanoparticle clusters[26]. The carbon layer could minimize the Mn dissolution effectively. The electrode-density and rate capability were also promoted due to the high electron conductivity of the carbon coating.

In this study, the core-shell structure $CF_x@C$ was prepared by microencapsulation and concentrated sulfuric acid carbonization. Polyurea was used as carbon precursor for its hydrophobicity and lipophobicity. Interfacial polymerization was adopted to form polyurea-coated CF_x microcapsule ($CF_x@P$) for insuring the independence of particles. The manufactured $CF_x@C$ shows a spherical shape and the carbon coating shows a porous surface. The material was tested as an cathode for lithium primary batteries, presenting high discharge capacity and excellent rate capability.

2. EXPERIMENTAL

2.1 Sample preparation

CF_x (x=1.0) was bought from Shanghai Carfluor Chemicals Co., Ltd. Isophorone diisocyanate (IPDI), alkyl phenol polyethylene glycol ether (OP-10) and polyvinyl alcohol (PVA) were all bought from Chengdu Xiya Chemical Technology Co., Ltd and used as prepolymer, dispersant, and emulsifier, respectively. Put 1.0 g IPDI, 0.5 mL OP-10 and 0.5 mL PVA in 50 mL water solvent to form slurry. Then added 1.0 g the CF_x powder into the slurry and stirred by a high-speed disperse

agitator with the rotate speed of 2000 rpm for 15 minutes to form a homogeneous oil-water emulsion. The encapsulation reaction was settled in the thermostatic waterbath of 40 ℃ for 8 hours with the stirring speed of 500 rpm and dibutyltin dilaurate (DBTDL) (Xiya Reagent) as catalyst. After filtrated and dried the products, the CF_x@P was prepared.

The carbonization of the CF_x@P was carried out in concentrated sulfuric acid with a magnetic stirring of 500 rpm for 12 h. Then the slurry was filtrated, and the filter residue was washed and dried in vacuum oven. Finally, the CF_x@C with a core-shell structure was obtained.

2.2 Structural characterization

The morphology was observed by MIRA3 TESCAN scanning electron microscopy (SEM) and JEM-2100 transmission electron microscopy (TEM). The X-ray diffraction (XRD) patterns were obtained using Ultima IV with Cu K_α radiation. The elemental analysis was carried out by the Oxford EDX analysis system. Fourier transform infrared (FTIR) spectrometer was test by infrared spectrophotometer JASCO Corporation FT/IR-300E.

2.3 Electrochemical measurements

The electrodes were composed of CF_x@C (70 *wt*.%), acetylene black (20 *wt*.%) to ensure electronic conductivity and polyvinylidene fluoride (10 *wt*.%) as binder. N-methyl pyrrolidone (NMP) was added to form uniform slurry. The cathode disks were transferred into an argon filled glove-box. The CR 2016 button cell was assembled after 8 h. A metallic lithium disk was used as the anode and a microporous polypropylene/polyethylene/polypropylene film was used as separator. The solution of 1 M $LiPF_6$ in ethylene carbonate (EC): dimethyl carbonate (DMC) (1:1, vol.) was employed as the electrolyte. Relaxation was performed for at least 12 h until open circuit voltage being stable. Galvanostatic discharges were carried out on a Neware battery test station, where 1 C rate equaled to 865 mA g^{-1} and the termination potential was 1.0 V.

3. RESULTS AND DISCUSSION

The morphology images of both CF_x and CF_x@C are showed in Fig. 1. The CF_x@C particles are individually displayed and shaped like spheres with the diameter of about 10 μm in Fig. 1a and Fig. 1b. The carbon coating is constructed of thousands of carbon micro-spheres with the diameter of about 0.2 μm. The carbon coating shows a porous surface which enlarges the specific surface and is benefit for storing electrolyte [25].
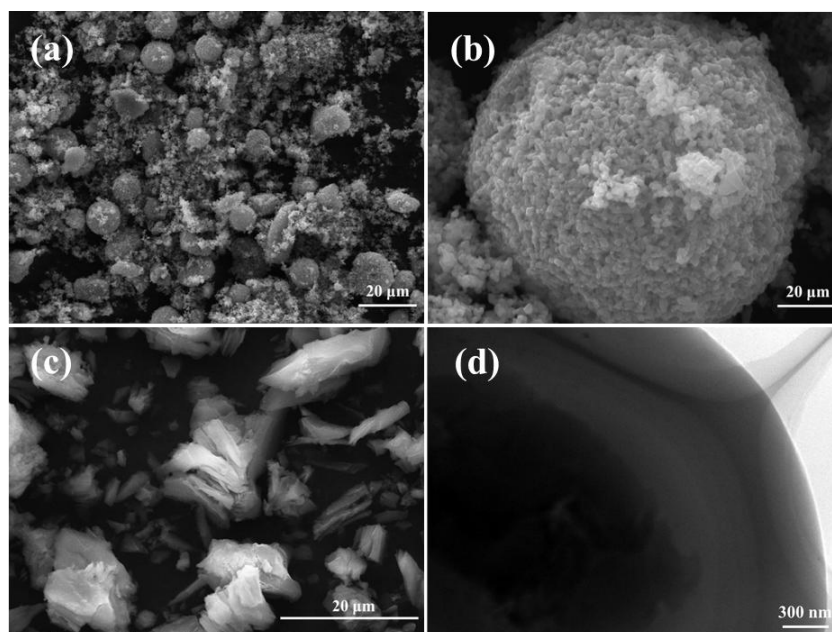
Figure 1. The morphology of graphite fluoride: (a and b) SEM images of $CF_x@C$, (c) SEM images of CF_x; (d) TEM image of $CF_x@C$.
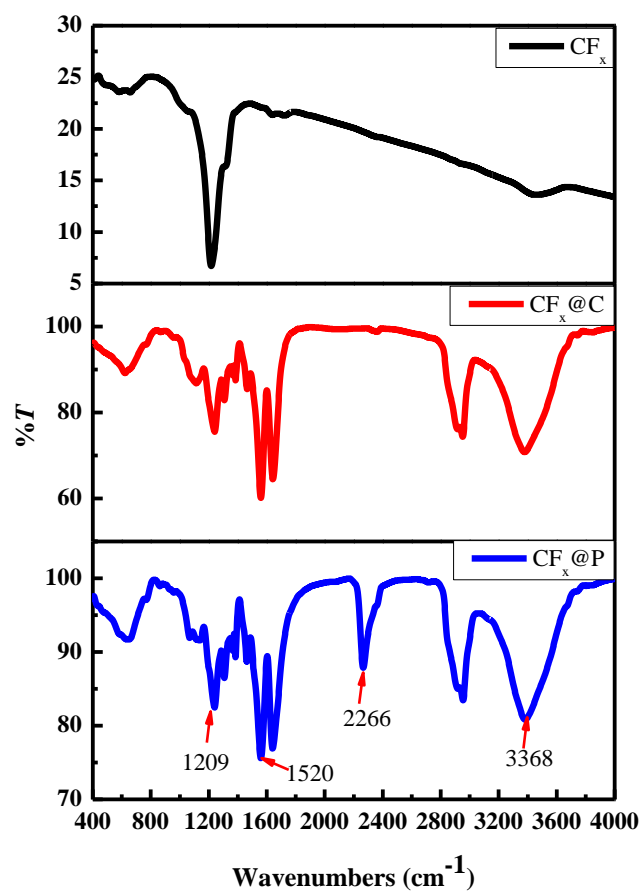

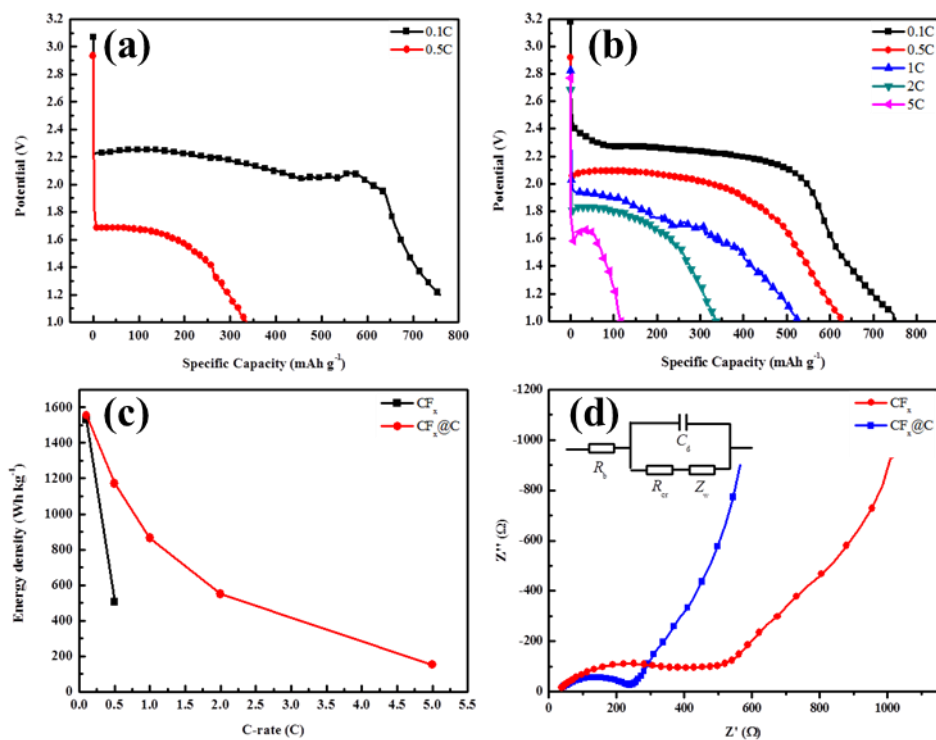**Figure 2.** FTIR spectra of different graphite fluorides.

Figure 3. Galvanostatic discharge curves of (a) CF_x and (b) $CF_x@C$; (c) Energy density by rates of both cells; (d) Impedance spectra of both cathodes.

Table 1. Electrochemical performances of both cells.

Samples	C-rate	Average Potential (E/V)	Specific Capacity (mAh g^{-1})	Energy density (Wh Kg^{-1})
CF_x	0.1 C	2.1	758	1503
	0.5 C	1.6	337	505
$CF_x@C$	0.1 C	2.2	747	1556
	0.5 C	2.0	630	1171
	1 C	1.7	527	864
	2 C	1.7	337	549
	5 C	1.6	115	173

The elemental analysis by EDX which is not shown here shows that there is about 20% increase in carbon mass percent from CF_x to $CF_x@C$, indicating there is really a carbon coating on the CF_x. In addition, the carbon has been coated on CF_x uniformly and the thickness of carbon layer is about 0.8 μm from the TEM image of $CF_x@C$, as shown in Fig. 1d.

The FTIR spectra of CF_x, $CF_x@C$ and $CF_x@P$ are showed in Fig. 2. The wave numbers of 3368 cm^{-1}, 2266 cm^{-1}, 1560 cm^{-1} and 1209 cm^{-1} are corresponding to the characteristic peaks of N-H, IPDI (N=C=O), polyurea, and C-F bonds, respectively. The peak at 2266 cm^{-1} is observed on the spectrum curve of $CF_x@P$, but vanishes on the spectrum curve of $CF_x@C$, which means there is some

IPDI left after polymerization process and the IPDI can be carbonized by concentrated sulfuric acid. However, as can be seen in Fig. 2, the feature peaks are observed at 3368cm^{-1} and 1560cm^{-1} on the spectrum curve of CF$_x$@C, demonstate that the polyurea cannot be completely carbonized by concentrated sulfuric acid. It is possible that the polyurea coating is too thick to be carbonized by concentrated sulfuric acid.

The galvanostatic discharge curves of CF$_x$ and CF$_x$@C at different current rates are presented in Fig. 3a and Fig. 3b. The electrochemical performances of CF$_x$ and CF$_x$@C cathodes are listed in Table 1 of which the average potential corresponds to the potential obtained at half the discharge. Fig. 3c shows the energy density as a function of discharge rate. It illustrates that the energy density and power density of CF$_x$@C cathode is remarkably higher than CF$_x$ cathode. The delivered specific capacity is very close between pristine CF$_x$ and CF$_x$@C when at 0.1 C. However, the rate capability has been greatly improved after coating. The CF$_x$@C cathode exhibits an excellent rate capability which can be steadily discharged at 2 C with an energy density of 549 Wh Kg^{-1}, in contrast with the pristine CF$_x$ cathode can only work until 0.5 C with an energy density of 505 Wh Kg^{-1}. Even at 5 C, the energy density can be delivered by 173 Wh Kg^{-1} for the CF$_x$@C cathode. The electrochemical performances of CF$_x$@C in this paper is very close to the carbon coated CF$_x$ in the former reports[22]. However, the pristine CF$_x$ in the former reports which can be discharged at 2 C is much better than the pristine CF$_x$ in this paper. On the whole, there is a greater improvement on CF$_x$@C in this paper.

Fig. 3d shows the room temperature Nyquist plots for fresh cells with CF$_x$@C and CF$_x$ cathodes. The symbols R_b, R_{cr}, C_d, and Z_w represent the volume resistance, battery reaction resistance, capacitance of the double layer, and Warburg impedance, separately. R_b is nearly the same for both cathodes which derives from the contacts of current collector, electrolyte, separator, and electrode. R_{cr} describes the interactions of the contact resistance between cathode particles, shell resistance, and charge transfer resistance, relevant to the depressed semicircle in the impedance plot. R_{cr} of CF$_x$@C cathode is much smaller than that of CF$_x$ cathode, indicating that the carbon coating on CF$_x$ improves the electrochemical performances significantly and reduces the contact resistance between particles.
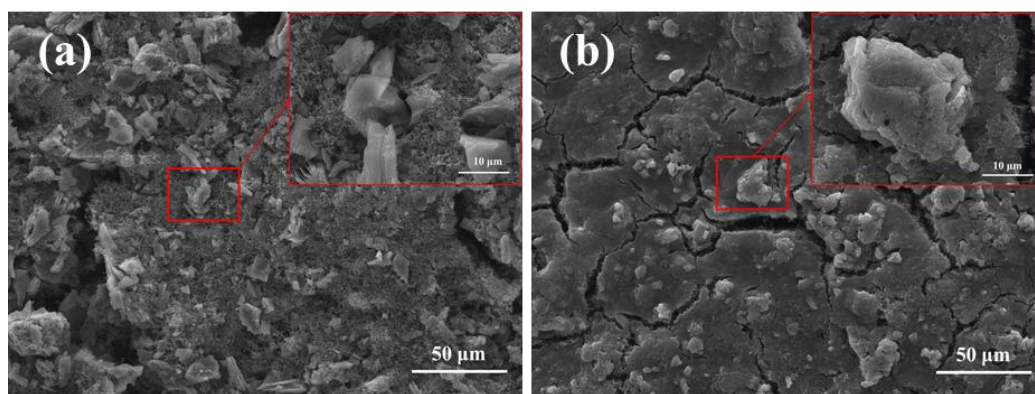

Figure 4. The SEM images of discharged graphite fluoride cathodes at 0.1 C: (a) CF$_x$ and (b) CF$_x$@C.
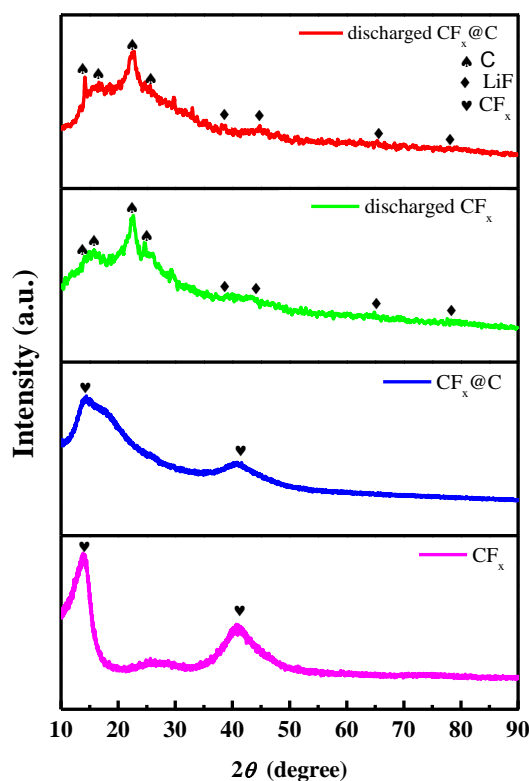
Figure 5. XRD patterns of the graphite fluorides and discharged cathodes.

To further reveal the discharge reaction, both fully discharged (at 0.1 C) pristin CF_x and $CF_x@C$ cathodes are studied by SEM and XRD (Fig. 4 and Fig. 5). As can be seen in Fig. 4a, the CF_x cathode presents a loosen structure and the combination between CF_x and acetylene black is weak. However, the $CF_x@C$ particles and acetylene black are tightly bonded, which guarantees the electrons transferring from Al collector to $CF_x@C$ particles (Fig. 4b). The $CF_x@C$ particles return to the irregularity shape of pristin CF_x from spherical shape. The enhanced combination of $CF_x@C$ cathode may be contributed to the polyurea left in the $CF_x@C$, for the polyurea can be dissolved in NMP and re-solidify as a binder.

Fig. 5 shows the XRD pattern of CF_x and $CF_x@C$ before and after discharge. The broad peak of $CF_x@C$ is wider than the CF_x, suggesting the existence of carbon coating. Because the carbonation has not totally done, leads to a low crystallinity of carbon layer which corresponds to a wider broad peak. In the XRD pattern of discharged cathode of CF_x and $CF_x@C$, both diffraction peaks corresponding to LiF and carbon are detected. So we can conclude that the main mechanism of electrochemical reaction for CF_x doesn't change by the carbon coating.

According to a widely accepted discharge reaction, there is a thin diffusion layer of a ternary graphite intercalation compound (GIC) during the discharge[4]. The GIC is decomposed by the subsequent reaction which maintains the thickness of diffusion layer to be a constant for a flat discharge potential. The GIC doesn't decompose to produce graphitic carbon until electrons transferred to the GIC interface from the current collector. For the $CF_x@C$ cathode, the electron transter has been

accelerated. Firstly, the enhanced combination of CF_x@C and acetylene black by plyurea guarantees the electrons transferring from Al collector to the surface of CF_x@C. And then, the carbon coating of CF_x@C with a good electronic conductivity accelerates the shift of electrons to the GIC interface. On the other hand, the carbon coating which shows a porous surface enlarges the contact area and can store much electrolyte and allows more channels for the Li^+ ion transferring. As a result, the discharge can get a fast reaction and the power density is increased.

4. CONCLUSIONS

The core/shell structure CF_x@C microcapsules have been manufactured by interfacial polymerization cladding polyurea and concentrated sulfuric acid carbonization. The particle connection and exterior conductivity for facile electron conduction are provided by the carbon layer. The energy can be discharged till 5 C for CF_x@C, but there is no capacity discharged at rates of higher than 0.5 C for CF_x. The high power density is attributed to: 1) the enhanced combination of CF_x@C and acetylene black by plyurea guarantees the electrons transferring from Al collector to the surface of CF_x@C; 2) the carbon coating of CF_x@C with a good electronic conductivity accelerates the shift of electrons to the GIC interface; 3) the carbon coating which shows an porous surface enlarges the contact area and can store much electrolyte and allows more channels for the Li^+ ion transferring.

The carbonization conditions and the thickness of carbon coating should be further optimized to enhance the electrochemical performances at high rates. Also the particle size of CF_x raw material should be reduced to provide a shorter length of lithium ion diffusion.

References

1. T. Nakajima, *J. Fluorine Chem.,* 149 (2013) 104.
2. M.A. Reddy, B. Breitung, M. Fichtner, *ACS Appl. Mater. Inter.,* 5 (2013) 11207.
3. T. Nakajima, V. Gupta, Y. Ohzawa, H. Groult, Z. Mazej, B. Žemva, *J. Power Sources,* 137 (2004) 80.
4. R. Hagiwara, *J. Electrochem. Soc.,* 135 (1988) 2128.
5. T. Nakajima, *J. Fluorine Chem.,* 105 (2000) 229.
6. R. Yazami, A. Hamwi, K. Guérin, Y. Ozawa, M. Dubois, J. Giraudet, F. Masin, *Electrochem. Commun.,* 9 (2007) 1850.
7. Y. Li, Y. Feng, W. Feng, *Electrochim. Acta,* 107 (2013) 343.
8. J. Giraudet, C. Delabarre, K. Guérin, M. Dubois, F. Masin, A. Hamwi, *J. Power Sources,* 158 (2006) 1365.
9. H. Touhara, F. Okino, *Carbon,* 38 (2000) 241.
10. P. Hany, R. Yazami, A. Hamwi, *J. Power Sources,* 68 (1997) 708.
11. R. Yazami, P. Hany, P. Masset, A. Hamwi, *Molecular Crystals and Liquid Crystals Science and Technology Section A,* 310 (1998) 397.

12. C. Delabarre, M. Dubois, J. Giraudet, K. Guérin, A. Hamwi, *Carbon,* 44 (2006) 2543.
13. Y. Sato, K. Itoh, R. Hagiwara, T. Fukunaga, Y. Ito, *Carbon,* 42 (2004) 3243.
14. Y. Li, W. Feng, *J. Power Sources,* 274 (2015) 1292.
15. P.J. Sideris, R. Yew, I. Nieves, K. Chen, G. Jain, C.L. Schmidt, S.G. Greenbaum, *J. Power Sources,* 254 (2014) 293.
16. J.Y. M. Nagata, M. Tomicsi, *ECS Trans,* 33 (2011) 223.
17. K. Guérin, R. Yazami, A. Hamwi, *Electrochem. Solid-State Lett.,* 7 (2004) A159.
18. H. Groult, C.M. Julien, A. Bahloul, S. Leclerc, E. Briot, A. Mauger, *Electrochem. Commun.,* 13 (2011) 1074.
19. S.S. Zhang, D. Foster, J. Read, *J. Power Sources,* 188 (2009) 601.
20. W. Yang, Y. Dai, S. Cai, Y. Zheng, W. Wen, K. Wang, Y. Feng, J. Xie, *J. Power Sources,* 255 (2014) 37.
21. S.S. Zhang, D. Foster, J. Read, *J. Power Sources,* 191 (2009) 648.
22. Q. Zhang, S. D'Astorg, P. Xiao, X. Zhang, L. Lu, *J. Power Sources,* 195 (2010) 2914.
23. H.C. Shin, W.I. Cho, H. Jang, *Electrochim. Acta,* 52 (2006) 1472.
24. W.M. Zhang, X.L. Wu, J.S. Hu, Y.G. Guo, L.J. Wan, *Adv. Funct. Mater.,* 18 (2008) 3941.
25. M. Rahman, J.Z. Wang, M.F. Hassan, D. Wexler, H.K. Liu, *Adv. Energy Mater.,* 1 (2011) 212.
26. S. Lee, Y. Cho, H.K. Song, K.T. Lee, J. Cho, *Angewandte Chemie,* 51 (2012) 8748.